Appl. Phys. B 71, 185–191 (2000) / Digital Object Identifier (DOI) 10.1007/s003400000370

**Applied Physics B**
Lasers
and Optics

# Limitations and guidelines for measuring the spectral width of ultrashort light pulses with a scanning Fabry–Pérot interferometer

**S. Marzenell, R. Beigang, R. Wallenstein**

Fachbereich Physik, Universität Kaiserslautern, Erwin-Schrödinger-Str., 67663 Kaiserslautern, Germany
(Fax: +49-631/205-3906, E-mail: marzenel@rhrk.uni-kl.de)

Received: 17 December 1999/Revised version: 14 April 2000/Published online: 5 July 2000 – 

**Abstract.** The measurement of the spectral width of ultrashort light pulses using a Fabry–Pérot interferometer (FPI) is investigated. It is shown, numerically and experimentally, that the measured width critically depends on the pulse properties (such as pulse shape, pulse duration, frequency chirp and wavelength) and on the properties of the FPI (such as the mirror spacing and the mirror reflectivities). The obtained results are of particular importance if the spatial length of the short light pulses is comparable or even shorter than the distance between the FPI mirrors. The derived guideline indicate that the actual spectral width of the ultrashort light pulses is measured with good accuracy only if the finesse $F \geq 40$ and the round trip time of the light pulses inside the Fabry–Pérot interferometer is approximately one to three times the pulse duration.

**PACS:** 06.60.J; 07.60.L

Ultrashort light pulses with pulse durations in the pico- or femtosecond regime are usually characterized by measuring their temporal and spectral width and by deducing from these data the time–bandwidth product. While the pulse duration is measured by using a fast photodiode, a streak camera or an autocorrelator the spectral width can be determined with a grating spectrometer or a Fabry–Pérot-type interferometer.

The spectral width of pulses with durations in the range of 10 fs to 1 ps (and a wavelength of for example 500 nm) is in the range of 0.4 nm to 40 nm. This broad spectrum can be measured with good accuracy using a grating spectrometer. For these ultrashort pulses techniques exist to determine both phase and amplitude, for example FROG. For longer pulses (1 ps to 100 ps) the spectral pulse width (of 0.4 nm to 0.004 nm) is much narrower. These widths are below the resolution limit of most grating spectrometers. It is thus more appropriate to use for example piezo-driven Fabry–Pérot spectrum analyzers. These devices offer the advantage that the free spectral range and the spectral resolution can be adjusted to the spectral pulse width by choosing an appropriate mirror spacing and mirror reflectivity. Whereas the spacing determines the free spectral range, the reflectivity determines the finesse, that is the ratio of the resolution-limited width of a transmission maximum to the free spectral range. Moreover the Fabry–Pérot interferometer (FPI) allows us to monitor on-line the pulse spectrum on for example an oscilloscope.

The purpose of the investigations reported in this paper is to determine the influence of the limited spatial pulse length on the spectral width as measured with a FPI of a given mirror spacing and reflectivity. The investigations include a numerical simulation of the dependence of the measured spectral pulse width on the pulse properties (such as pulse shape, pulse duration, frequency chirp and wavelength) as well as on the properties of the FPI (such as mirror spacing and the finesse, calculated from the mirror's reflectivity). The results obtained by these calculations are then verified in an experimental investigation in which the spectral width of Fourier-limited 50-ps-long pulses of a mode-locked Nd:YLF laser is measured with a FPI using different mirror spacings.

An interferometer with a limited number of interfering waves described in the literature is for example the Lummer–Gehrcke interferometer [1]. The response of a FPI to short light pulses was investigated in respect to interpulse interference effects [2] and pulse stretching [3]. More general calculations of the response of a FPI to short pulses were performed in the time domain [4–6].

Both, the time and frequency response of a Fabry–Pérot interferometer to short light pulses have been considered so far only in a qualitative way [7, 8] or are calculated for rectangular and $\mathrm{sinc}^2$-shaped pulses [9]. A corresponding method to FROG for time-resolved spectral measurements based on a Fabry–Pérot interferometer is described and modeled for rectangular pulses [10]. But there are no quantitative results that describe the influence of a short pulse duration on the width of the measured spectrum for Gaussian and $\mathrm{sech}^2$-shaped pulses. This is the subject of the investigations reported here.

## 1 Numerical simulation of the measured spectral pulse width

The intensity $I(\phi)$ transmitted by a scanning Fabry–Pérot interferometer is given by the Airy formula

$$I(\phi) = \frac{\mathcal{T}}{1 + \mathcal{F}\sin^2(\phi/2)}\,, \tag{1}$$

where $\mathcal{T} = [T/(1-R)]^2$, $\mathcal{F} = 4R/(1-R)^2$, $T$ and $R$ are flux transmittance and reflectance, respectively, $\phi = 4\pi d/\lambda$, $d$ is the mirror spacing and $\lambda$ the wavelength. For a limited number $m$ of interfering waves the transmission $I(\phi)$ is approximately given by [7]

$$I_m(\phi) = \left|\sum_{n=0}^{m-1} TR^n \mathrm{e}^{\mathrm{i}n\phi}\right|^2 . \tag{2}$$

$I$ is equal to $I_m$ if $m \to \infty$. For a short pulse $m$ is given by the number of round trips in the Fabry–Pérot interferometer. For a mirror spacing $d$ the round trip time is simply

$$t_0 = 2d/c\,.$$

For a pulse with duration $\tau$ the number of round trips is given by

$$m = \tau c/2d\,.$$

If $m$ is larger than $\approx 2F$, i.e. twice the value of the total finesse $F$, the value of $I$ given by (1) and the approximate value $I_m$ are almost equal. If $m$ is larger than twice the value of the finesse, the measured spectrum should be the same for pulsed or continuous wave (cw) radiation [7]. The finesse $F$, which is proportional to the FPI's resolving power, is defined as the ratio of the free spectral range to the half-width of the Airy curve.

With a decreasing number of round trips, that is for shorter light pulses, the difference between $I_m$ and $I$ increases. The precise knowledge of this difference should allow us to determine the spectral width also for pulses with a spatial pulse length comparable to the FPI's mirror separation. In the following this difference and the required correction factor for the measured spectral shape are calculated.

In the simulation the transmission of a scanning Fabry–Pérot interferometer is calculated by considering the propagation of a single pulse within the Fabry–Pérot interferometer with fixed mirror spacing. The transmitted pulse power is then calculated for other mirror spacings in order to obtain the complete spectrum of the pulse.

In the following we consider Gaussian and sech$^2$-shaped pulses which are typical for ultrashort pulses generated by actively or passively mode-locked lasers. The temporal envelope of these pulses is given by the following expressions:

$$f_\tau^{\mathrm{gaus}}(t) = \exp\left(-2\ln 2 \times t^2/\tau^2\right)\,, \tag{3}$$

$$f_\tau^{\mathrm{sech}}(t) = \mathrm{sech}(1.763 \times t/\tau)\,, \tag{4}$$

where $\tau$ is the full width at half maximum (FWHM) of the pulse duration.

The calculation is started at the time $-t_\mathrm{s}$ when the pulse intensity is at a level of $10^{-3}$ of its maximum and stopped at $t_\mathrm{s}$ when the intensity has decreased by the same factor (see Fig. 1). The pulse duration is divided into intervals which correspond to the round trip time $t_0$ in the Fabry–Pérot interferometer.

Starting at the time $-t_\mathrm{s}$ only one beam leaves the Fabry–Pérot interferometer during the first round trip. Therefore the transmitted intensity $I_1(d)$ can be calculated using (2) with $m = 1$:

$$I_1(d) = \left|\int_{-t_\mathrm{s}}^{-t_\mathrm{s}+t_0(d)} T f(t)\,\mathrm{d}t\right|^2 = T^2\left|\int_0^{t_0(d)} f(t-t_\mathrm{s})\,\mathrm{d}t\right|^2 . \tag{5}$$

After the second round trip two beams have left the Fabry–Pérot interferometer, one beam which is only transmitted and one beam which was reflected twice inside the Fabry–Pérot interferometer. These two beams must be taken into account in (2) with $m = 2$, the corresponding phase relation $\phi$ and an amplitude given by the pulse shape $f(t)$. The resulting intensity $I_2(d)$ is then given by

$$I_2(d) = \left|\int_{-t_\mathrm{s}}^{-t_\mathrm{s}+t_0(d)} \left\{TR\mathrm{e}^{\mathrm{i}\phi(d)} f(t) + T f(t+t_0(d))\right\}\mathrm{d}t\right|^2$$

$$= T^2 \times \left|\int_0^{t_0(d)} \left\{R\mathrm{e}^{\mathrm{i}\phi(d)} f(t-t_\mathrm{s}) + f(t-t_\mathrm{s}+t_0(d))\right\}\mathrm{d}t\right|^2 . \tag{6}$$

This procedure is repeated until the pulse propagated $m$-times in the FPI and $-t_\mathrm{s} + mt_0(d) > t_\mathrm{s}$. In this case the recorded intensity is given by

$$I_m(d) = T^2 \times \left|\int_0^{t_0(d)} \sum_{n=0}^{m} R^n \mathrm{e}^{\mathrm{i}n\phi(d)} f(t - t_\mathrm{s} + mt_0(d) - nt_0(d))\,\mathrm{d}t\right|^2 . \tag{7}$$

After the tail of the pulse has passed the first FPI mirror no additional light will enter the FPI. The energy stored at this time inside the FPI will leave the interferometer because of the

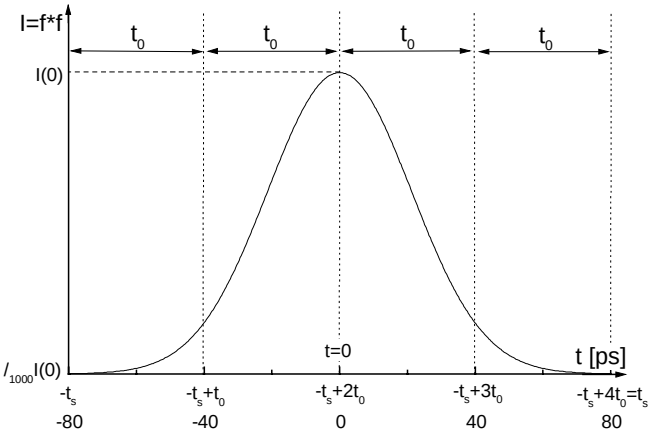


**Fig. 1.** Pulse of 50 ps length divided into intervals which correspond to the round trip time in an air-spaced Fabry–Pérot interferometer with a mirror separation of 6 mm

small but finite mirror transmission. Additional losses caused by absorption, scattering or by misalignment are not taken into account. The finesse of this Fabry–Pérot interferometer is thus determined only by the reflectivity of the mirrors. In order to calculate the fading of the energy stored in the FPI the sum given by (7) has to be modified. After each round trip start and stop values of the sum are increased by 1, thus the sum starts at $n = 1, 2, \ldots, j, \ldots$ instead of $n = 0$ and ends at $m+1, m+2, \ldots, m+j, \ldots$ with a constant difference of $m$. To simplify this expression, the contributions of the increasing powers of $R$ are separated. The rest of the sum remains constant which is equal to (7) with an additional factor of powers of $R$. This is given by

$$
\begin{aligned}
&I_{m+j}(d) = T^2 \times \\
&\left| \int_0^{t_0(d)} \sum_{n=j}^{m+j} R^n \mathrm{e}^{\mathrm{i}n\phi(d)} f(t - t_\mathrm{s} + mt_0(d) + jt_0(d) - nt_0(d)) \,\mathrm{d}t \right|^2 \\
&= R^{2j} T^2 \times \\
&\left| \int_0^{t_0(d)} \sum_{n=0}^{m} R^n \mathrm{e}^{\mathrm{i}n\phi(d)} f(t - t_\mathrm{s} + mt_0(d) - nt_0(d)) \,\mathrm{d}t \right|^2 \\
&= R^{2j} I_m(d) \,. \qquad (8)
\end{aligned}
$$

For the calculation of the total transmitted intensity for a given mirror separation $d$ all summands $I_i$ ($i \to \infty$) have to be added, i.e. until the light intensity in the Fabry–Pérot interferometer is zero. In this case $I(d)$ is given by

$$
\begin{aligned}
I(d) = \sum_{i=1}^{\infty} I_i(d) &= \sum_{i=1}^{m-1} I_i(d) + \sum_{i=m}^{\infty} I_i(d) \\
&= \sum_{i=1}^{m-1} I_i(d) + \sum_{i=0}^{\infty} I_m(d) R^{2i} \\
&= \sum_{i=1}^{m-1} I_i(d) + I_m(d) \frac{1}{1-R^2} \,. \qquad (9)
\end{aligned}
$$

This sum can be written as a sum of $m$ different terms. The first part stands for the increase of energy while the pulse enters the Fabry–Pérot interferometer whereas the second part describes the decrease of the stored energy at times larger than $t_\mathrm{s}$ (8).

Equation (9) gives the intensity for a fixed spacing $d$. By varying the distance $d$ the transmission of the Fabry–Pérot interferometer is obtained as a function of $d$. The distance between two successive transmission maxima corresponds to the free spectral range. Thus the transmission of the Fabry–Pérot interferometer can be described also as a function of frequency.

The parameters that have to be known for the calculation are the reflectivities of the mirrors, the wavelength, the pulse duration, the temporal pulse shape, a possible frequency chirp and the mirror separation. The calculation performed for a successively increasing mirror separation then provides the transmission maxima, the distance between two adjacent maxima and the full width at half maximum (FWHM). The calculated FWHM is the parameter of interest, that is the spectral width $\Delta\nu$ of the light pulse.

With this procedure the spectral width of Gaussian and sech$^2$-shaped pulses were investigated using the following parameters: The mirror spacing was $d = 100\,\mu\mathrm{m}$, varied by $\pm 3.5\,\mu\mathrm{m}$. The mirror distance of $100\,\mu\mathrm{m}$ corresponds to a round trip time of $t_0 = 667\,\mathrm{fs}$. The free spectral range is $\nu_\mathrm{FSR} = 1.5\,\mathrm{THz}$. The center wavelength of the pulses was $\lambda = 5\,\mu\mathrm{m}$. The pulse duration was varied from 0.15 ps to 60 ps.

The results of the numerical calculations are shown in Figs. 2 and 3 for Gaussian and in Figs. 4 and 5 for sech$^2$-shaped pulses, respectively. In addition, relevant data are listed in Tables 1 and 2 for the two different pulse shapes. In Figs. 2 and 4 the normalized spectral width $\Delta\nu/\nu_\mathrm{FSR}$ is plotted as a function of the normalized pulse length $\tau/t_0$ for different values of the finesse $F$. The solid diagonal line in each figure represents the spectral width of Fourier-limited pulses. Using the normalized parameters allows a more general discussion of the results obtained for different values of the pulse length, the finesse and the free spectral range.

The time–bandwidth product is calculated by multiplying the spectral width $\Delta\nu$ with the corresponding pulse duration $\tau$. The dependence of $\tau\Delta\nu$ on the normalized pulse

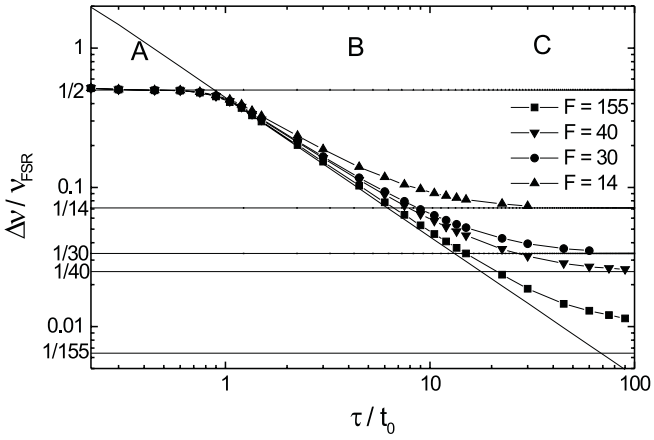


**Fig. 2.** Ratio of the spectral width ($\Delta\nu$) to the free spectral range ($\nu_\mathrm{FSR}$) in dependence of the ratio of the duration ($\tau$) of Gaussian pulses to the round trip time ($t_0$) calculated for different values of the finesse ($F$)

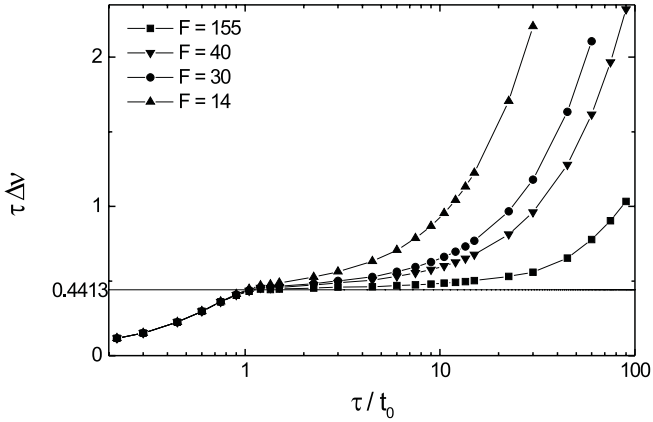


**Fig. 3.** Time–bandwidth product ($\tau\Delta\nu$) in dependence of the ratio of the duration ($\tau$) of Gaussian pulses to the round-trip time ($t_0$) calculated for different values of the finesse ($F$)

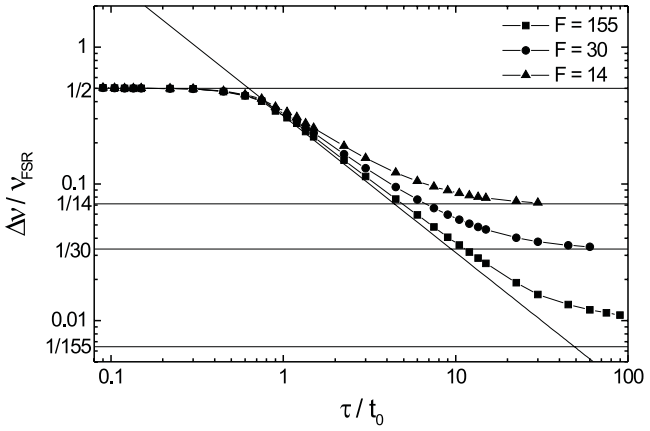


**Fig. 4.** Ratio of the spectral width ($\Delta\nu$) to the free spectral range ($\nu_{FSR}$) in dependence of the ratio of the duration ($\tau$) of sech$^2$-shaped pulses to the round-trip time ($t_0$) calculated for different values of the finesse ($F$)

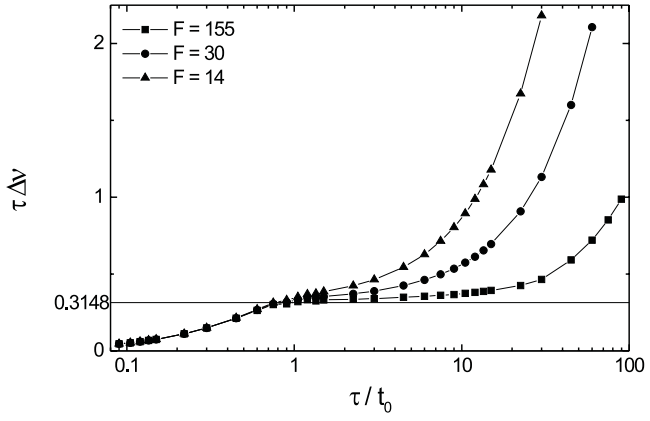


**Fig. 5.** Time–bandwidth product ($\tau\Delta\nu$) in dependence of the ratio of the duration ($\tau$) of sech$^2$-shaped pulses to the round-trip time ($t_0$) calculated for different values of the finesse ($F$)

duration ($\tau/t_0$) is shown in Figs. 3 and 5 for different values of the finesse $F$.

As seen in Fig. 2 for pulses that are short compared to the Fabry–Pérot round-trip time (area A) the ratio $\Delta\nu/\nu_{FSR}$ does not depend on the finesse $F$. If the pulse duration is less than 20% of the round-trip time the pulse is simply reflected at the two surfaces of the Fabry–Pérot interferometer and no interference occurs. With $I_0$ the intensity of the input pulse, the transmitted intensity is given by $T^2/(1-R^2)\times I_0$. Because there is no interference, it is not possible to determine a spectral width. If the pulse duration increases but

**Table 1.** Values of the ratio of the spectral width ($\Delta\nu$) to the free spectral range ($\nu_{FSR}$) and the time–bandwidth product ($\tau\Delta\nu$) calculated for Gaussian pulses and different values of the finesse ($F$)

| | $F=155$ | | $F=30$ | | $F=14$ | |
|---|---|---|---|---|---|---|
| $\tau/t_0$ | $\frac{\Delta\nu}{\nu_{FSR}}$ | $\tau\Delta\nu$ | $\frac{\Delta\nu}{\nu_{FSR}}$ | $\tau\Delta\nu$ | $\frac{\Delta\nu}{\nu_{FSR}}$ | $\tau\Delta\nu$ |
| 0.45 | 0.497 | 0.224 | 0.497 | 0.224 | 0.497 | 0.224 |
| 1.50 | 0.297 | 0.446 | 0.309 | 0.464 | 0.325 | 0.487 |
| 4.50 | 0.103 | 0.461 | 0.117 | 0.528 | 0.140 | 0.631 |
| 15.00 | 0.0335 | 0.503 | 0.0513 | 0.770 | 0.0813 | 1.22 |
| 45.00 | 0.0145 | 0.654 | 0.0363 | 1.63 | 0.0718 | 3.23 |

**Table 2.** Values of the ratio of the spectral width ($\Delta\nu$) to the free spectral range ($\nu_{FSR}$) and the time–bandwidth product ($\tau\Delta\nu$) calculated for sech$^2$-shaped pulses and different values of the finesse ($F$)

| | $F=155$ | | $F=30$ | | $F=14$ | |
|---|---|---|---|---|---|---|
| $\tau/t_0$ | $\frac{\Delta\nu}{\nu_{FSR}}$ | $\tau\Delta\nu$ | $\frac{\Delta\nu}{\nu_{FSR}}$ | $\tau\Delta\nu$ | $\frac{\Delta\nu}{\nu_{FSR}}$ | $\tau\Delta\nu$ |
| 0.15 | 0.499 | 0.075 | 0.499 | 0.075 | 0.499 | 0.075 |
| 0.45 | 0.473 | 0.213 | 0.475 | 0.214 | 0.477 | 0.215 |
| 1.50 | 0.221 | 0.332 | 0.236 | 0.355 | 0.257 | 0.385 |
| 4.50 | 0.0773 | 0.349 | 0.0947 | 0.426 | 0.121 | 0.544 |
| 15.00 | 0.0262 | 0.393 | 0.0463 | 0.695 | 0.0787 | 1.18 |
| 45.00 | 0.0131 | 0.592 | 0.0355 | 1.60 | 0.0715 | 3.22 |

is still shorter than the round-trip time only those parts of the pulses will contribute to the interference with intensities less than half the pulse maximum. The transmitted average intensity is still in the order of $T^2/(1-R^2)\times I_0$, but the constructive or destructive interference of the pulse wings leads to some modulation of the transmitted intensity as a function of mirror spacing $d$. This results in a very low contrast ratio. The calculated spectra look like a sine function with the zero-line at $T^2/(1-R^2)\times I_0$ and with a period of the free spectral range. Therefore the ratio of $\Delta\nu$ to $\nu_{FSR}$ is $1/2$. This value is indicated in Figs. 2 and 4 by the upper horizontal line.

For longer pulse widths (area B) the numerically determined spectral width is correct until the spectral width expected for a Fourier-limited pulse is smaller than the resolving power of the FPI (area C). For large values of $\tau/t_0$ the measured spectral width is equal to the resolving power and is independent of the pulse length. In Figs. 2 and 4 the values of the resolving power determined by the finesse are drawn as horizontal lines. As a result with a Fabry–Pérot interferometer the correct spectral width can be measured only if $\tau/t_0 \approx 1$. The upper tolerable limit of $\tau/t_0$ depends on the accuracy required in the measurement. For example for a ratio of $\tau/t_0 = 5$ and a finesse $F = 30$ the measured spectral width will deviate by 20% from the width of the assumed Fourier-limited pulses. With increasing finesse this deviation decreases. If the finesse is increased to 155, for example, the deviation is reduced to 5% for the same ratio of $\tau/t_0$. Therefore the accuracy required in the measurement limits the maximum value allowed for the ratio of $\tau/t_0$.

Figures 3 and 5 show the time–bandwidth product $\tau\Delta\nu$ given by the spectral width $\Delta\nu$ (determined from the numerical simulation) and the pulse duration $\tau$. The horizontal lines are drawn at a value of 0.4413 and 0.3148, which are the Fourier limits for $\tau\Delta\nu$ for Gaussian and sech$^2$-shaped pulses, respectively. For short pulses ($\tau/t_0 < 1$) the values for $\tau\Delta\nu$ are independent of the finesse. The determined value of the time–bandwidth product is smaller than the Fourier limit. For intermediate values of the ratio $\tau/t_0$ ($1 < \tau/t_0 < 3$) the value for $\tau\Delta\nu$ is rather accurate, whereas for longer pulses the value is too large. In this case the resolving power of the Fabry–Pérot interferometer is too small to resolve the narrow spectrum of the longer pulses. The time–bandwidth product thus increases with increasing pulse length because the spectral pulse width remains constant because it is equal to the value of the resolving power. This result indicates that the range in which the Fabry–Pérot interferometer could be used critically depends on the finesse $F$.

In the simulation only the finesse as calculated from the reflectivity $R$ ($F_R = \pi\sqrt{R}/(1-R)$) is considered. The finesse of real Fabry–Pérots is smaller due to for example mirror surface distortion, mirror misalignment, scattering losses, and absorptions in the mirror coatings, etc. The contributions of these effects which reduce the finesse could be considered, however, in the calculation. The total finesse $F$ is then given by the equation $1/F^2 = 1/F_R^2 + \sum 1/F_i^2$, where $F_i$ are the contributions by the effects mentioned above [11]. On the other hand the reduced value of the finesse can be considered in the calculations simply by assuming an appropriate reduced mirror reflectivity. In this way the results obtained by the numerical simulation and in the experiment can be directly compared. The effective finesse is determined experimentally in a measurement with a small mirror spacing, which results in a large ratio of pulse duration to Fabry–Pérot round-trip time. In this case the measured spectral width is only determined by the finesse and is equal to the free spectral range divided by this finesse.

Since the results are presented as a function of the normalized pulse duration $\tau/t_0$ and the normalized spectral width $\Delta\nu/\nu_{\mathrm{FSR}}$ they are valid for pulses with durations in the whole temporal range extending from ns to fs.

Besides Fourier-limited pulses Gaussian pulses with linear frequency chirp were investigated. The parameters chosen for the numerical simulations were the same as those used for the calculations shown in Fig. 2 ($d = 100\,\mu\mathrm{m}$, $\lambda = 5\,\mu\mathrm{m}$, $0.15\,\mathrm{ps} < \tau < 60\,\mathrm{ps}$, $F = 30$). The chirp factor $a$ for a linear chirp is defined by the following equation [12]:

$$E(t) = E_0 \exp\left(-t^2/2T^2\right) \cos\left(\omega t + \frac{at^2}{T^2}\right) . \tag{10}$$

The chirp factor $a$ was varied between 0 and 20. The time–bandwidth product of a chirped Gaussian pulse depends on the chirp factor $a$ and can be calculated with a Fourier transformation. The result is

$$\Delta\nu\Delta\tau = 0.4413\sqrt{1+4a^2} . \tag{11}$$

The numerical simulations were performed in the same way as for chirp-free pulses. The chirp is considered in (7) and (8) by an additional term in the phase $\phi(d)$. The results of the numerical calculations are shown in Fig. 6 for chirp factors $a$ in the range of 0 to 20. For increasing values of $a$ the normalized spectral pulse width increases. The general behavior, however, characterized by starting horizontally at a value of $1/2$, decreasing linearly and leveling off horizontally at a value of $1/30$, corresponds to the results shown in Fig. 2 for chirp-free pulses.

In order to allow an easy comparison with Fourier-limited pulses an effective pulse duration can be defined as

$$\tau_{\mathrm{eff}} = \frac{\tau}{\sqrt{1+4a^2}} . \tag{12}$$

If this pulse duration is used the dependence of $\Delta\nu/\nu_{\mathrm{FSR}}$ is the same for all chirp factors (as is seen from Fig. 7). Using the effective pulse duration it is thus possible to determine the optimum mirror spacing required for a reliable measurement of the spectral width of pulses with known duration $\tau$ and frequency chirp factor $a$.

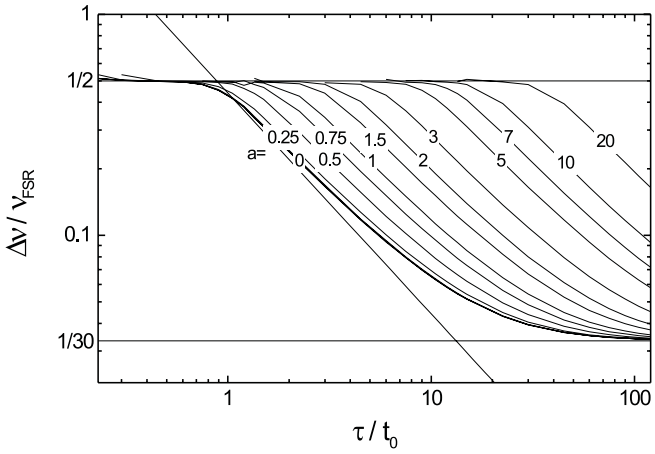


**Fig. 6.** Ratio of the spectral width ($\Delta\nu$) to the free spectral range ($\nu_{\mathrm{FSR}}$) in dependence of the ratio of the duration ($\tau$) of Gaussian pulses to the round-trip time ($t_0$) calculated for values of the chirp factor ranging from $a = 0$ to $a = 20$

In general, it is desirable to use a Fabry–Pérot interferometer with a high finesse. At a finesse of 30 the mirror spacing should be set to a length that a pulse performs 1 to 3 round trips. If the pulse is chirped, however, the effective pulse duration is shorter compared to a pulse without chirp. In this case the ratio of the effective pulse duration to Fabry–Pérot round-trip time would be smaller than 1 and the measurement would result in a wrong value for the spectral width. This can be avoided by decreasing the mirror spacing.

## 2 Experimental investigation

To compare the calculated results with measured data the spectral width of ps pulses from a cw mode-locked Nd:YLF laser (repetition rate 75.4 MHz, wavelength 1053 nm, pulse duration 50 ps ± 10%) was measured for several mirror spacings with a home-built scanning Fabry–Pérot interferometer. The mirror spacing was increased in steps from 55 μm to 8890 μm. In this way the spectral width was measured and

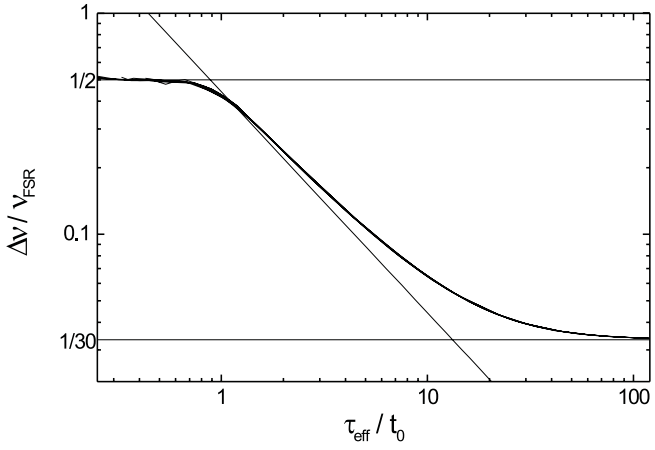


**Fig. 7.** Ratio of the spectral width ($\Delta\nu$) to the free spectral range ($\nu_{\mathrm{FSR}}$) in dependence of the ratio of the effective duration ($\tau_{\mathrm{eff}}$) of Gaussian pulses to the round-trip time ($t_0$) calculated for the same values of the chirp factor as given above

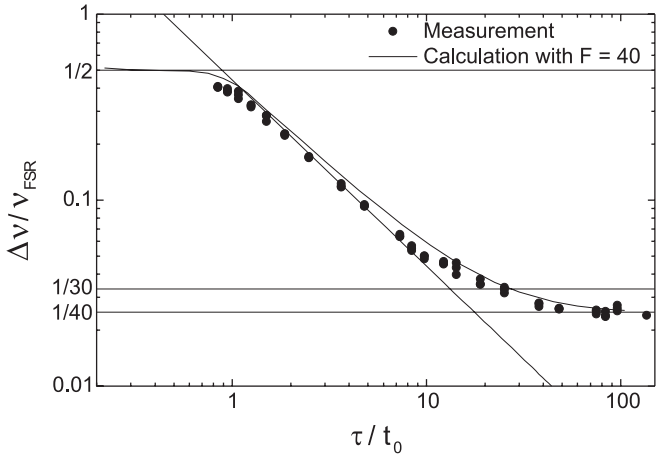


**Fig. 8.** Ratio of the measured spectral width ($\Delta\nu$) to the free spectral range ($\nu_{FSR}$) in dependence of the ratio of the 50-ps-long pulses from a Nd:YLF laser to the round-trip time ($t_0$) (for details: see text)

analyzed for 22 different mirror spacings. The obtained experimental values are shown in Fig. 8. This figure shows in addition a horizontal line at a ratio of the spectral width to the free spectral range of 1/2, a horizontal line at the resolving power for a finesse of 30 and a horizontal line at the resolving power for a finesse of 40. Furthermore a line indicates the ratio of the spectral width to the free spectral range as calculated from the product $\Delta\nu\Delta\tau = 0.4413$ for a pulse duration of 50 ps and mirror spacings of 0.25 mm to 15.0 mm which provide a ratio of $\tau/t_0$ from 0.5 to 30. The experimental values are compared with the data of a numerical simulation assuming a finesse of 40.

At small mirror spacings which provides values of the ratio $\tau/t_0 \geq 10$, the measured spectral width equals the resolving power of the Fabry–Pérot interferometer. With increasing mirror spacing (decreasing value of $\tau/t_0$) the measured results are close to the spectral width calculated from the time–bandwidth-product. At large mirror spacing ($\tau/t_0 < 1$) the measured values approach the constant value of 1/2 as the calculations predict. All measured data are slightly shifted to smaller values of $\tau/t_0$. This cannot be explained by uncertainties in the determination of the mirror spacing. However, an increase of the duration of the Nd:YLF laser pulses by 10% could account for this shift. In fact, increasing the value for the pulse duration from 50 ps to 55 ps which is in the range of the error of the determination of the pulse duration resulted in a very good agreement between the measured and the calculated spectral pulse widths.

## 3 Discussion

The results from the numerical simulation and their good agreement with measured data allow us to calculate the optimum mirror spacing of a Fabry–Pérot interferometer for measuring the spectral width of short light pulses. The mirror spacing should be chosen such that the ratio of effective pulse duration and Fabry–Pérot round-trip time is between 1 and 3. In this case the measured spectral width is nearly independent of the finesse of the Fabry–Pérot interferometer (see for example Fig. 2) and the difference between the measured and the actual spectral width is minimized. If the finesse is known accurately any value between 1 and 10 or even higher can be chosen. For a chirp-free pulse or a small frequency chirp ($a \leq 1$) and a known pulse length (determined by an autocorrelation measurement) only a ratio between pulse length and round-trip time in the range of 1 to 3 should be used in order to measure the spectral width with no or only a small error.

The results from the numerical simulation are also useful to measure the spectral width of chirped pulses and to determine the chirp factor using the following procedure: First the pulse duration is measured and the finesse of the Fabry–Pérot interferometer has to be determined. To measure the finesse, the mirror separation should be as small as possible. The measured spectral pulse width of the pulses is then equal to the free spectral range divided by the finesse. Then the mirror separation of the Fabry–Pérot interferometer is increased to one to three times the spatial pulse length. If the spectral width measured with such mirror separation is equal or close to half of the free spectral range, the pulse is strongly chirped (see Fig. 6). The mirror separation has thus to be reduced until the measured spectral width is 0.2 times the free spectral range. In this case the ratio between the effective pulse length $\tau_{\text{eff}}$ and the Fabry–Pérot interferometer round-trip time $t_0$ is 2.25 (see Fig. 7). From the measured spectral width the ratio between the effective pulse length and Fabry–Pérot interferometer round trip time can be determined from Figs. 7, 2 or 4 depending on the finesse and the pulse shape. With the use of (12) the unknown chirp factor $a$ can be obtained and equation (11) provides the time–bandwidth-product.

Because the measured spectral width depends on the finesse of the FPI and on the number of round trips of the light pulses in the Fabry–Pérot resonator the measured spectral width can be different from the spectral width calculated from the time–bandwidth product (see (11) and Fig. 2). In order to obtain the actual width a correction factor which depends on the pulse duration $\tau$, pulse chirp $a$, mirror spacing $d$, finesse $F$ and pulse shape has to be applied. This correction factor is shown in Fig. 9 for Gaussian pulses in dependence of the ratio $\tau_{\text{eff}}/t_0$ and for different values of the finesse $F$. The measured spectral width has to be divided by this correction factor to obtain the actual spectral width.

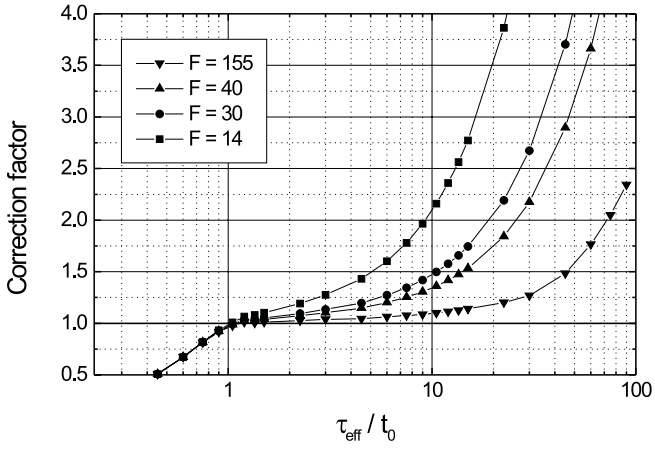


**Fig. 9.** Correction factor between the measured and the actual spectral width in dependence of the ratio of the effective duration ($\tau_{\text{eff}}$) of Gaussian pulses to the round-trip time ($t_0$) calculated for different values of the finesse ($F$)

## 4 Conclusion

Guidelines and limitations for the use of a scanning Fabry–Pérot interferometer for the measurement of the bandwidth of ultrashort light pulses have been presented. The spectral response of a scanning Fabry–Pérot interferometer is numerically simulated taking into account the pulse shape, the mirror spacing, the pulse duration and the mirror reflectivities. These simulations are performed also for chirped pulses. The results indicate that the actual spectral width of the ultrashort light pulses is measured with good accuracy only if the finesse $F \geq 40$ and the round-trip time of the light pulses inside the Fabry–Pérot interferometer is approximately one to three times the pulse duration.

## References


1. M. Born, E. Wolf: *Principles of Optics* (Pergamon Press, Oxford 1975)
2. W.E. Martin, D. Milam: Appl. Opt. **15**, 3054 (1976)
3. W.E. Martin: Opt. Commun. **21**, 8 (1977)
4. A. Kastler: Nouv. Rev. Opt. **5**, 133 (1974)
5. C.A. Eldering, A. Dienes, S.T. Kowel: Opt. Eng. **32**, 464 (1993)
6. B.J. Offrein, H.J.W.M. Hoekstra, J.P. van Loenen, A. Driessen, Th.J.A. Popma: Opt. Commun. **112**, 253 (1994)
7. C. Roychoudhuri: J. Opt. Soc. Am. **65**, 1418 (1975)
8. G. Cesini, G. Guattari, G. Lucarini, C. Palma: Opt. Acta **24**, 1217 (1977)
9. H. Daussy, R. Dumanchin, O. de Witte: Appl. Opt. **17**, 451 (1978)
10. M.G. Davis, R.F. O'Dowd: Opt. Eng. **33**, 3937 (1994)
11. W. Demtröder: *Laser Spectroscopy* (Springer, Berlin, Heidelberg, New York 1982)
12. K.L. Sala, G.A. Kenney-Wallace, G.E. Hall: IEEE J. Quantum Electron. **QE-16**, 990 (1980)